Proceedings of Global Power and Propulsion Society
ISSN-Nr: 2504-4400
GPPS Hong Kong 2023
October 17-19, 2023
www.gpps.global

GPPS-TC-2023-226

IN-SITU PERFORMANCE OF AXIAL FLOW FAN FOR AIR-COOLED CONDENSERS

Alessandro Corsini
Dept. of Mechanical and Aerospace Engineering, Sapienza University of Rome
alessandro.corsini@uniroma1.it
Rome, Italy

Giovanni Delibra
Dept. of Mechanical and Aerospace Engineering, Sapienza University of Rome
giovanni.delibra@uniroma1.it
Rome, Italy

Johan van der Spuy
Dept. of Mechanical and Mechatronic Engineering, Stellenbosh University
sjvdspuy@sun.ac.za
Stellenbosh, South-Africa

Lorenzo Tieghi
Dept. of Mechanical and Aerospace Engineering, Sapienza University of Rome
lorenzo.tieghi@uniroma1.it
Rome, Italy

ABSTRACT

Here we present a study on a fan for air-cooled condensers installed in Stellenbosh University test rig. It is a 7.3m diameter fan operated at 151 rpm and installed in a facility that, due to the presence of a channel below the structure and nearby buildings naturally operate with non-uniform inflow. This rises concerns about the inflow conditions that the fan can experience, leading to the present investigation to quantify possible disuniformities at the fan inlet. For this reasons several flow conditions are analysed to address this issue along the fan curve, providing a comparison with respect to measured (electric) power. Also the manuscript address how the flow develops downstream of the fan, to characterize the wake velocity defect at the inlet of the ACC heat exchanger.

INTRODUCTION

Air-cooled condensers are devices commonly found in power plants situated in regions with limited access to water resources. These condensers employ air as the working fluid for the essential heat exchange process required for condensation to take place [1]. The combination of these two factors naturally results in ACC to be present in Concentrated Solar Power plants, due to their desert installations. To facilitate the movement of air, large arrays of condenser units are utilized, each equipped with one or more low-speed axial fans with diameters spanning several meters. Depending on the power plant's layout, various unit configurations can be employed, based on factors such as fan placement (upstream or downstream) or the geometry of the tube bundle (V- or A-shaped). However, regardless of the configuration, these units are all designed to operate in open atmospheric conditions [2].

In such conditions, ACCs often encounter off-design situations caused by factors like ambient temperature fluctuations, daily variations, lateral winds, wind gusts, obstructions from surrounding structures, or a combination of these elements [3]. Due to the significant number of units involved and their individual power requirements, off-design operations can lead to a substantial increase in auxiliary power demand [4]. To mitigate the impact of external factors on ACC performance, potential strategies focus on optimizing the ACC layout within the power plant and/or enhancing the fans' robustness to off-design conditions and inflow distortions. For instance, Butler and Grimes [2] emphasized the necessity of considering historical local ambient wind conditions during the preliminary design of the condenser layout.

In this study, the in-situ performance of an air-cooled condenser (ACC) fan installed in the Stellenbosh University test rig for air-cooled condensed are investigated. This fan has a diameter of 7.3 meters and operates at a speed of 151 rpm and was designed, manufactured and installed in a real-scale ACC facility under the H2020 Minwater Project [5], Figure 1. The installation site, characterized by a channel below the structure and nearby buildings, naturally experiences non-

uniform inflow conditions. This manuscript focuses on numerical simulations of the actual facility arrangement, comparing the performance of a reference fan with CFD data. By analyzing the pressure and efficiency curves of both setups, we aim to understand the impact of the installation setup on the fan performance and in particular to address the effects of the lateral walls that partially obstruct the setup inflow and that of the channel that flows under the fan inflow.

FAN AND FACILITY SPECIFICATIONS

The test facility is a full-size ACC installation in the Stellenbosch University campus and is shown in Figure 1. The fan (here labelled as MFan and shown in Figure 1 and 2) is installed 6.5 m above the ground, with an orizontal channel flowing underneath. Given the fan size (Table 1) the setup is quite unique, as from the specification table (Table 1) this is characterized by a duty point at very high flow rate (333 m^3/s) and negligible static pressure rise (117 Pa). Also, given the typical installation of these setups it is extremely difficult to control the tip-gap of the device, that has a nominal value of 3.68 cm.

Figure 1. ACC Facility (left) and axial fan (right)

Table 1. Axial fan design specifications

tip radius	3.680 m
tip clearance	36.8 mm
hub-to-tip ratio	0.29
rotational speed	151 rpm
tip section Reynolds nr = $\frac{D_{tip}V_{tip}}{\nu}$	38.5 M
fan Reynolds nr = $\frac{DV_{tip}}{\nu}$	28.5 M
number of blades	8
volumetric flow rate	333 m^3/s
static pressure rise	117 Pa
design power	57 kW

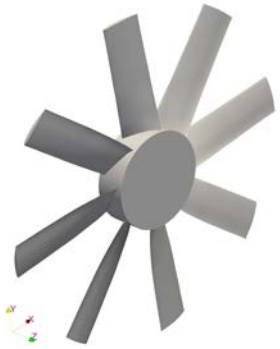

Figure 2. Model of the MFan

METHODOLOGY

A sketch of the computational domain and boundaries is shown in Figure 3. The volumetric flow rates of the fan were imposed and equally split between the two inlets. The inlets turbulent intensity was set to 2%, and the dissipation rate was computed accordingly. Solid surfaces were assigned a no-slip boundary condition, utilizing the high Reynolds wall function for turbulent quantities. The lateral and top surfaces were treated as slip surfaces to ensure numerical stability. Neumann boundary conditions were applied for all quantities at the outflow.

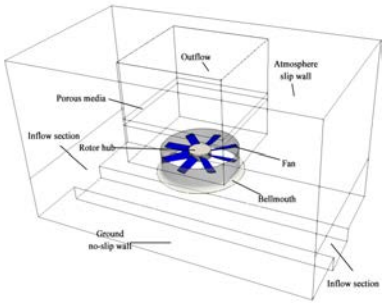

Figure 3. Computational domain and boundary conditions

Commentato [GD1]: This portion of the text was moved upstream according to Reviwer 3, point 3

Incompressible Navier-Stokes equations were solved using OpenFOAM-v21 with a stationary SIMPLE solver. The relative motion between fan and the environment was accounted for using the Multiple Reference Frame (MRF) approach, while the grid upstream of the fan and the heat exchanger downstream of the fan were modelled as a porous medium according to Darcy-Forchheimer law **Errore. L'origine riferimento non è stata trovata.**. The porous medium is placed 1D downstream of the fan, to model the straightener, tuning the Darcy-Forchheimer coefficients to provide a pressure drop of 40 Pa (according to measurements) at the design volume flow rate.Turbulence modeling relied on RANS approach with RNG k-ε model. The interaction between the blades and the flow was solved employing a frozen rotor approach, where the Navier-Stokes equations were solved in a Moving Reference Frame (MRF).

The computational grids were generated using the OpenFOAM *snappyHexMesh* built-in utility, starting from a background grid with isotropic cells of 0.2 m, and successive refinements based on the grid sensitivity analysis presented in **Errore. L'origine riferimento non è stata trovata.**. The final total grid count is of 18 million cells, tuned for high Reynolds number calculations with a target y^+ value of 100 in the tip region of the fan. As the straightener is simulated using a porous media approach, no grid refinement is necessary in the chamber. Highlights of the computational grid are shown in Figure 4.

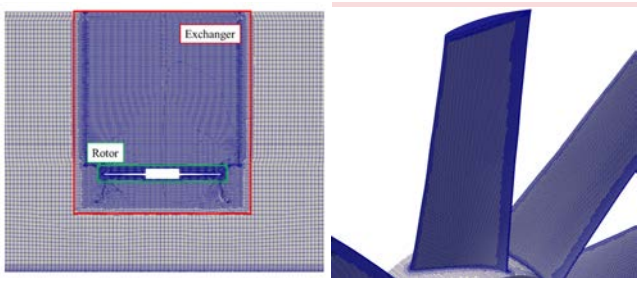

Figure 4. Highlights of the computational grid: left: meridional plane, right: rotor blades

Commentato [GD2]: This figure was added to comply to issues highlighted by Rev. 1 and 3

RESULTS AND DISCUSSION

Integral performance and validation

CFD data at design point result in a pressure rise of the MFan equal to 100 Pa, showing a discrepancy of 17 Pa with respect to the design point of the fan measured in ISO 5801 conditions on a 1.5 m model and then scaled to full-size. This discrepancy of course accounts for the installation layout and the impossibility of using the same measurement section in the real layout. Unfortunately it is not possible to currently measure the pressure performance in the test rig, but only to measure electric power. The comparison of CFD data, accounting for a 96% electric efficiency at design point and 92% reduction at lower flow rate is shown in Figure 5. Agreement is fairly good and previous works on the same setup lead to the conclusion that also pressure rise is correctly reproduced.

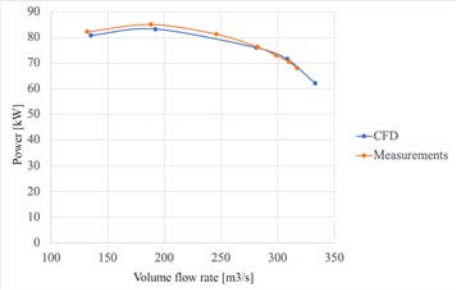

Figure 5. Elecric Power curve measured vs CFD.

Commentato [GD3]: Labels were added to this figure

Effects of lateral walls and underneath channels on the inflow conditions.

Contours of axial and peripheral velocities in the bellmouth section of the fan are shown in Figure 6, that is placed 1.5 m upstream of the fan chord midspan section (see Figure 3). In this figure, the downstream channel flows from left to right. The figure shows fields for 92.5%, 58% and 40% of the design flow rate operations. Axial velocity contours (top row) show that in this section the flow field is fairly symmetric in azimuthal direction, leading to the conclusion that the fan is not affected by the asymmetry coming from the underneath channel and the lateral buildings. There is, however, an impact of the boundary layer developing on the bellmouth and a low-velocity region in the center that is the effect of the downstream fan hub, especially at the lower flow rate. Contours of swirl velocity component (bottom row) lead to conclude that also in this case the asymmetry in the computational domain do not affect the inflow velocity field. Thus, preliminary concerns about the installation effects of the facility in the space confined between adjacent buildings seem to be overcome.

Commentato [GD4]: An error was corrected

In Figure 7 axial (top) and peripheral (bottom) velocity component contours are shown for two sections 1.5 m (left) and 4.0 m (right) downstream of the fan. The first was cut at the maximum shroud radius to better follow the wake dynamics, the latter shows the full section 20 cm upstream of the porous medium that simulates the heat exchanger. At 92.5% of the design flow rate the axial velocity contour shows a significant influence of the wake released by the 8 blades and a central core with recirculating flow, in the wake of the fan hub. Reducing the flow rate of the fan at 58% and 40% of the design flow rate the hub recirculation that in the first section extends up to ¾ of the area. Moving 2 m downstream, just before the inflow of the heat exchanger, the wake further mixes reducing the overall velocity defect. In the case of 92.5% of the flow rate a zone of recirculation extends along the four sides of the squared duct, with a residual recirculation in the center downstream of the fan hub. Reducing the flow rate the recirculation along the side walls reduces, however the central part of the section is characterized by negative axial velocity, so it is still negatively affected by the wake of the fan hub. Residual swirl in both sections show a significant effect only at the higher flow rate, that in the second considered cross-section seem strictly related to the sidewalls recirculation.

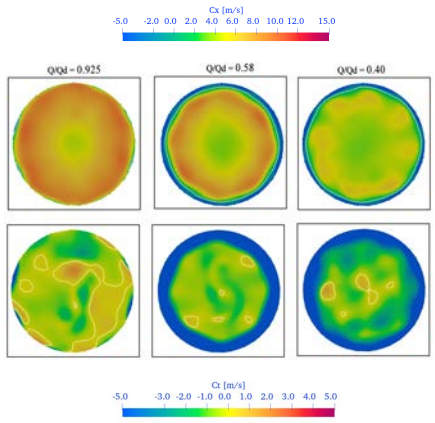

Figure 6. Axial (top row) and peripheral (bottom row) velocity 1.5 m upstream of the MFan (bellmouth section) at different flow rates. White line contour corresponds to zero value for the considered velocity component.

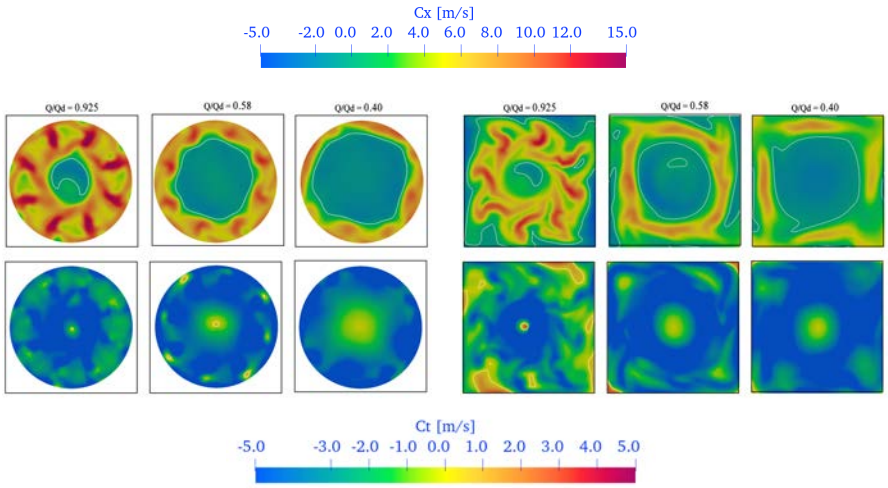

Figure 7. Axial (top row) and peripheral (bottom row) velocity 1.5 m (left) and 4.0 m (right) downstream of the MFan at different flow rates. White line contour corresponds to zero value for the considered velocity component.

CONCLUSIONS

Numerical computations of the Stellenbosh ACC facility were carried out in OpenFOAM to address concerns about the presence of nearby buildings and a channel that flows underneath the fan, to identify possible distortions of the inlet conditions in absence of lateral wind. A secondary research question was about the characterization of the flow field at ther inlet of the heat exchanger, to address concerns about the air-flow disuniformities downstream of the fan. Results of computations, here validated against electric power measurements on the facility, show that the fan inflow is not affected by the lateral buildings nor the underneath channel. The only significant disuniformities are in fact due to the presence of the fan hub and the restriction resulting from the passage to the fan duct to the annulus. These are hardly easy to overcome

with a more aerodynamic hub nose due to the dimensions of the device and the additional weight required by further material. In the section downstream of the fan, however, velocity distribution is strongly affected by the abrupt cutting of the fan hub, with a central recirculating region that is still not recovered at the heat exchanger inlet. This effect is particularly strong at lower flow rates, raising concerns on heat exchange capabilities in these cases.

ACKNOWLEDGMENTS

This project has received funding from the European Union's Horizon 2020 research and innovation programme under grant agreement No. 654443.

REFERENCES

[1]. Astolfi, M.; Martelli, E.; Pierobon, L. 7 - Thermodynamic and technoeconomic optimization of Organic Rankine Cycle systems. In 286 Organic Rankine Cycle (ORC) Power Systems; Macchi, E.; Astolfi, M., Eds.; Woodhead Publishing, 2017; pp. 173–249. 287

[2]. Butler, C.; Grimes, R. The effect of wind on the optimal design and performance of a modular air-cooled condenser for a 288 concentrated solar power plant. Energy 2014, 68, 886–895.

[3]. Marincowitz, F.; Owen, M.; Muiyser, J. Multi-objective optimisation for wind resistant air-cooled condenser operation. Applied 290 Thermal Engineering 2023, 218, 119382. 291

[4]. Chen, L.; Yang, L.; Du, X.; Yang, Y. A novel layout of air-cooled condensers to improve thermo-flow performances. Applied Energy 292 2016, 165, 244–259.

[5]. https://minwatercsp.eu (last accessed on 26th May 2023)

[6]. Tieghi L; Delibra G; van der Spuy J; Corsini A. Leading Edge Bumps for Flow Control in Air-Cooled Condensers. International Journal of Turbomachinery, Propulsion and Power. 2023; 8(1):9.

APPENDIX A - COPYRIGHT/OPEN ACCESS